

# A Comparative Study of Frequency Ratio (FR) and Logistic Regression (LR) in Landslide Susceptibility Mapping for Cebu Province, Philippines

Azel Mae A. Sañez<sup>1</sup>, Jayson L. Arizapa<sup>2</sup>, Jenielyn T. Padrones<sup>2</sup>, Cristina L. Tiburan Jr.<sup>2</sup>

<sup>1</sup>College of Forestry and Natural Resources, University of the Philippines Los Baños - aasanez@up.edu.ph

<sup>2</sup>Institute of Renewable Natural Resources, College of Forestry and Natural Resources, University of the Philippines Los Baños - {jlarizapa1, jtpadrones, ctiburan}@up.edu.ph

**Keywords:** hazard assessment, geographic information system, area under curve, predictive modelling, receiver operating characteristics, landslide susceptibility index

## Abstract

Landslides rank as one of the most damaging natural disasters occurring in the Philippines, particularly in geologically and climatically complex regions such as Cebu Province. Accurate landslide susceptibility mapping is crucial for reducing disaster risks and promoting sustainable land use planning. This research evaluates the effectiveness of two commonly applied statistical models—Frequency Ratio (FR) and Logistic Regression (LR)—in producing landslide susceptibility maps for Cebu Province. Seven environmental conditioning factors were analyzed: slope, elevation, aspect, topographic wetness index (TWI), topographic position index (TPI), soil texture, and curvature. Landslide inventory data from 2009 to 2023 were compiled from news reports and validated using Google Earth imagery. Both FR and LR models were applied using the same set of factors, and their predictive performances were evaluated using ROC-AUC curve. Results show that both models effectively delineate landslide-prone areas, with slope emerging as the most influential factor. The LR model demonstrated marginally higher predictive accuracy with AUC of 0.9151 compared to the FR model with AUC of 0.8955, due to its ability to account for multivariate interactions among factors. The map produced by LR was compared to the existing map from MGB, and 257,142.11 hectares were found to fall within the agreement zone, having the same classification. The resulting susceptibility maps provide a scientific basis for local government units to enhance disaster preparedness, guide land use decisions, and prioritize risk mitigation efforts in Cebu Province.

## 1. Introduction

A landslide involves the downward displacement of soil, rock, or debris along a slope, representing a natural phenomenon that has significantly influenced the formation of many areas of the Earth's surface (Vasudevan and Ramanathan, 2016). Although landslides have positive impacts on the ecological aspect, this phenomenon is considered one of nature's most destructive disasters (Shabbir et al., 2022). Each year, landslides result in numerous fatalities, injuries, and substantial economic damages by devastating infrastructure, properties, businesses, farmlands, highways, and transportation routes (Shabbir et al., 2022).

The Philippines is one of the most hazard-exposed countries (Bolletino et al., 2018). Its location on several plate boundaries and inside typhoon belt brings frequent floods, typhoons, landslides, earthquakes, volcanic activity and drought (Bolletino et al., 2018). It experiences some of the highest rates of rainfall-triggered landslides in Southeast Asia, with hydrological hazards causing thousands of fatalities and extensive economic losses annually (Jones et al., 2023). These are further exacerbated by anthropogenic activities such as illegal logging and kaingin. Landslides occur due to both natural and human factors. Weather, soil type, slope and vegetation play a role, while construction, logging, and urban growth increases their chances.

To address landslide risk, various research in the Philippines use several landslide susceptibility methods (Arizapa, et al., 2015; Jones et al., 2023). These methods include the Analytic Hierarchy Process (AHP), weighted overlay, logistic regression analysis, and frequency ratio, each offering unique insights into landslide-prone areas by modelling correlations between landslide events and factors such as slope, geology, land use etc using Geographic Information System (GIS). However, most of these studies are concentrated in the northern regions of the country, particularly in Luzon. This uneven research distribution

leaves provinces such as Cebu which is equally prone to landslides underrepresented in susceptibility mapping literature.

Effective landslide mitigation and management depend on accurate susceptibility assessments, which evaluate the likelihood of landslides based on spatial probability (Shano et al., 2020). These assessments are crucial for disaster risk reduction, supporting post-disaster recovery, and guiding urban development (Chang et al., 2023). In Cebu, where rapid urbanization intersects with environmentally sensitive terrain, there is an urgent need for updated and reliable landslide susceptibility maps. Through susceptibility mapping, local authorities gain essential tools for land use planning and determining areas appropriate for future growth (Chang et al., 2023). This study applies FR and LR methods to develop a landslide susceptibility map of Cebu Province, thereby addressing the limited research outside Luzon and advancing geomatics-based approached for disaster risk reduction in the Central Philippines.

## 2. Methodology

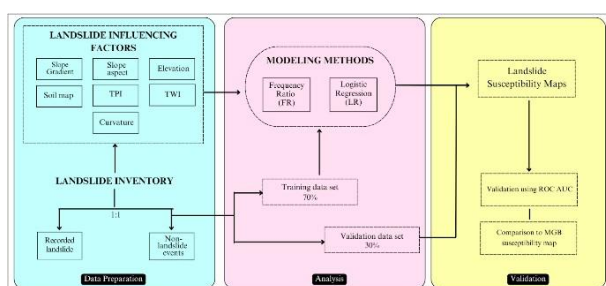


Figure 1. Methodological framework of the study.

The study used GIS and statistical models to build landslide susceptibility maps. Frequency Ratio and Logistic Regression measured how landslide events relate to seven key factors: slope, aspect, elevation, soil texture, topographic position index, topographic wetness index, and curvature.

## 2.1 Study Site

The research is carried out in Cebu Province, a long and narrow island featuring rolling hills and rugged mountain terrains. According to the Department of Environment and Natural Resources–Mines and Geosciences Bureau (DENR-MGB), these areas are characterized by steep slopes, intense weathering, predominantly non-cohesive soils, and weak rock strength. Common indicators of active movement include surface cracks, bulging ground, step-like terraces, and water seepage (Garas, 2013 as cited by Beroya-Eitner et al., 2023). Furthermore, the MGB ranks Cebu eighth among the top ten provinces in the Philippines most prone to landslides.

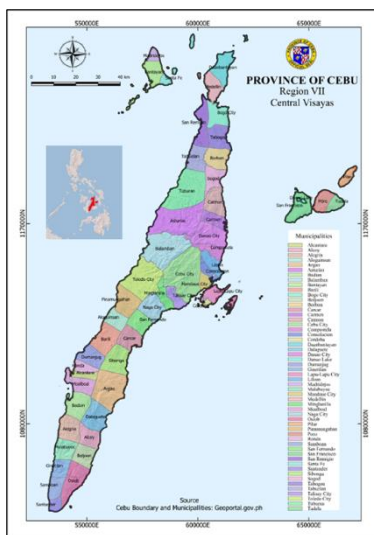


Figure 2. Location and boundary of Cebu Province.

## 2.2 Landslide Inventory

Historical landslide inventory data is usually lacking in the country. Unlike floods, unless there are casualties, landslides occurrences are usually not documented especially those that occurred in remote areas. This study employed a systematic approach using Google Earth which have been widely used in collecting historical landslide data in the absence of historical landslide data (Chang et al., 2023). The use of Google Earth's historical and high-resolution satellite images has become a widely accepted and effective approach for landslide inventory mapping, enabling the detection and digitization of both large and smaller, localized landslides that are often underreported in broader datasets. In addition, to ensure reliability of the collected landslide data, collection date was time based on significant rainfall events and news reports articles and reports from the Department of Social Welfare and Development's Disaster Response Operations Monitoring and Information Center (DSWD DROMIC) of the region. Additionally, the collected landslide information were cross-checked with the existing landslide hazard map of MGB for the region and ensure that these landslide data fall in the highly susceptible landslide areas.

The study was able to collect a total of 130 landslide polygons distributed across the province of Cebu. These landslide data were used to develop and train the model. To avoid bias and

firmly evaluate the predictive performance of the model, 130 non-landslides polygons were generated. Following the approach of Fu et al. (2025) to reduce the risk of misclassifying unstable slopes or undetected landslides as non-landslide samples - a common source of bias - each identified landslide was buffered by 500 meters, and non-landslide points were only selected outside these buffer zones. This is done emphasize the importance of maintaining spatial separation between landslide and non-landslide samples to enhance model accuracy and reduce uncertainty. Lastly, the collected landslide and non-landslide data were divided into training and testing data using a 70:30 ratio.

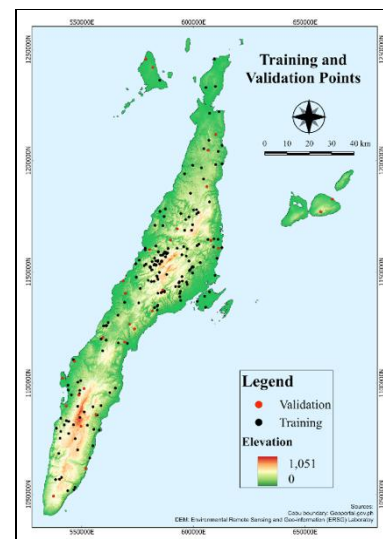


Figure 3. Landslide inventory map.

## 2.3 Landslide Causative Factors

Factor selection is a crucial part of landslide susceptibility study, but no universal standard exists, as choices vary with data availability (Wubalem, 2021). Given data limitations in Cebu Province, this study used static factors—elevation, slope, aspect, curvature, topographic position index (TPI), topographic wetness index (TWI), and soil texture—which capture terrain and geological predispositions independent of transient triggers (Liao et al., 2022). Elevation influences rainfall, vegetation, and soil development (Sharma & Sandhu, 2024) and was classified into five equal-interval classes (0–1051 m). Slope governs gravitational stress (Cellek, 2020) and was grouped into six categories following the National Land Use Committee standard, with the largest area falling under 30–50%. Aspect affects solar radiation, wind, and rainfall (Gorokhovich & Vustianuk, 2021) and was classified into nine categories following ESRI. General curvature, which regulates water flow and moisture retention, was classified into concave, flat, and convex based on Zaslavsky & Sinai (1981) and Moore et al. (1993) as described by Blaga (2012).

TWI, which reflects topographic control on soil moisture and pore pressure, was divided into five categories—very dry, dry, medium, wet, and very wet—following Meles et al. (2019). TPI, used to identify landform positions such as ridges, valleys, and slopes, was classified into five classes based on Weiss (2001). Finally, soil texture, which governs infiltration, drainage, and cohesion (Temme, 2021), was sourced from NAMRIA via the Philippine Geoportal and grouped into six classes: clay, beach sand, clay loam, silt loam, hydrosol, and undifferentiated soil type.

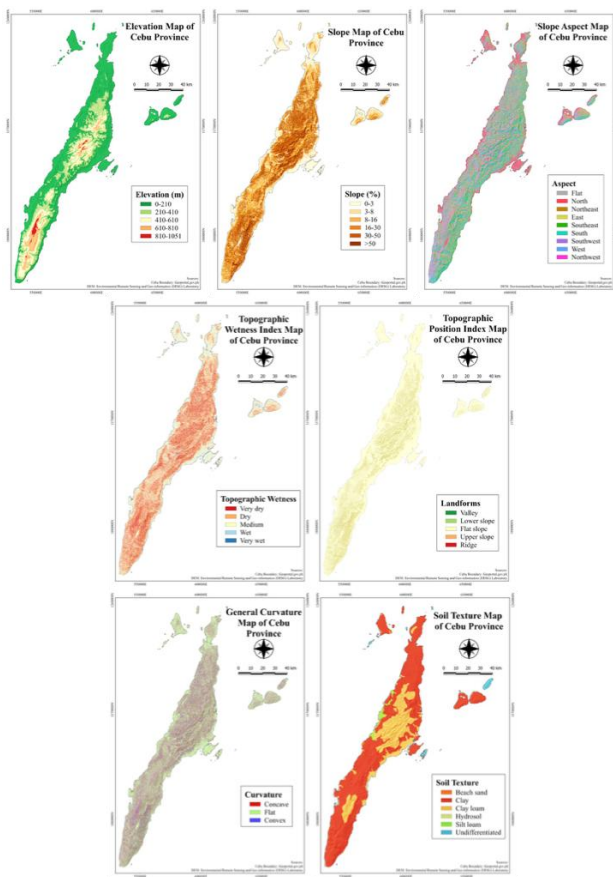


Figure 4. Causative factors in landslide susceptibility mapping.

## 2.4 Modeling Techniques

### 2.4.1 Frequency Ratio (FR)

The frequency ratio (FR) method is a straightforward bivariate statistical approach which yields accurate results, making it popular for landslide susceptibility mapping (Silalahi et al., 2019). Mathematically, FR is expressed as:

$$FR = \frac{Npix(si) / Npix(Ni)}{\sum_i Npix(si) / \sum_i Npix(Ni)} \quad (1)$$

where:  $Npix(Si)$  = pixels marked as landslide in parameter class i

$Npix(Ni)$  = overall count of landslide pixels in the area

$\sum_i Npix(Si)$  = pixel count for parameter i

$\sum_i Npix(Ni)$  = total pixels in the study area

A frequency ratio above 1 indicates a strong and positive association with landslides and a higher chance of occurrence. Conversely, if the frequency ratio is below 1, it implies a weak or negative relationship between landslide occurrences and the data class, indicating a low landslide probability, while a ratio of 1 signifies an average relationship. Once the frequency ratios are calculated, all the raster maps' frequency ratio parameters are summed to form the Landslide Susceptibility Index (LSI) as defined by Equation 2 wherein high value represents areas more prone to landslides, and low values mark areas less likely to experience them.

$$LSI = \sum_{i=1}^n FRi \quad (2)$$

where:  $n$  = number of landslide causal factors

$Fri$  = Frequency ratio of pixels of landslide factors

### 2.4.2 Logistic Regression

Logistic regression provides an effective technique for assessing how landslide occurrences depend on key factors (Das and Lepcha, 2019). This uses dichotomous variables (e.g., 1 for present and 0 for not) with outcomes shaped by one or more predictors. As a generalized linear model, its probability is computed by the following equation:

$$P = \frac{1}{(1+e^{-z})} \quad (3)$$

where:  $P$  = likelihood of landslide on a 0 to 1 scale

Values closer to 1, it indicates high vulnerability, and values closer to 0, it indicates very low vulnerability.  $z$  represents the linear predictor of the model expressed as:

$$z = b_0 + b_1 x_1 + b_2 x_2 + \dots + b_n x_n \quad (4)$$

where:  $b_0$  = model intercept

$n$  = number of independent variables

$b_1, b_2 \dots b_n$  = regression coefficients

$x_1, x_2 \dots x_n$  = factors contributing to landslides

## 2.5 Validation Methods

ROC curve analysis was used to evaluate the model's accuracy. The area under the ROC curve (AUC) serves as the main measure for determining model accuracy. The diagonal from (0,0) to (1,1) marks random guessing and corresponds to  $AUC = 0.5$ . Curves that rise further above this line have higher AUCs and better performance. AUC values lie from 0.5 to 1, with 1 representing a perfect model.

The AUC are grouped into five classes: 0.9-1 (excellent), 0.8-0.9 (very good), 0.7-0.8 (good), 0.6-0.7 (moderate) and 0.5 – 0.6 (bad) (Umbara, 2024). ROC curve and its AUC are widely accepted standards to evaluate the effectiveness of landslide susceptibility models, as demonstrated in previous studies (Sun et al., 2018; Umbara, 2024).

$$AUC = \sum_{i=0}^n (x_i - x_{i-1}) y_i - \left[ \frac{x_i - x_{i-1}}{2} (y_i - y_{i-1}) \right] \quad (5)$$

where:  $x_i$  = percentage of the area

$y_i$  = area of the landslide

## 3. Results and Discussion

### 3.1 Application of Frequency Ratio

The FR model identified slopes greater than 50% as having the highest frequency ratio value of 4.36, indicating a strong correlation between steep slopes and landslide occurrences. This finding aligns with Sheng et al. (2022), who highlighted slope steepness as a primary factor influencing landslide susceptibility. Similarly, Zézere et al. (2017), as cited by Sonker et al. (2021), emphasized that increasing slope angles exacerbate slope instability, thereby raising the likelihood of landslides. The TPI also supports this trend; wherein the upper slope class exhibited a high FR value of 4.40. These results underscore the universal importance of slope steepness as a critical conditioning factor for landslides, both locally and globally.

In addition to slope, soil characteristics play a significant role in landslide susceptibility in Cebu Province. While slope influences

the shear stress within soil masses, soil type governs shear strength and permeability, affecting stability under saturated conditions (Kinde et al., 2024). The FR model revealed that clay loam soils have a strong association with landslide events (FR = 3.05). Similar findings were observed by Cabelin and Jadina (2019) in Cadac-an Watershed, Leyte, where loam to clayey textures, characterized by low bulk density, and high porosity contribute to instability in landslide-prone. This interplay of soil composition and drainage dynamics regulates infiltration rates, pore water pressure, and slope stability was comprehensively explored by Yao et al. (2025).

Classes	FR	Classes	FR	Classes	FR
Soil Texture		Slope (%)			TPI
Beach sand	0.00	0-3	0.00	Valley	0.00
Clay	0.37	3-8	0.01	Lower slope	2.43
Clay loam	3.05	8-16	0.04	Flat slope	0.94
Hydrosol	0.00	16-30	0.21	Upper slope	4.40
Silt loam	0.00	30-50	0.59	Ridge	0.00
Undifferentiated	0.00	>50	4.36		
Aspect		Elevation (m)		TWI	
Flat	0.22	0-210	0.33	Very dry	2.09
North	0.00	210-410	1.95	Dry	1.18
Northeast	1.97	410-610	3.16	Medium	0.40
South	1.26	610-810	0.96	Wet	0.09
East	0.75	810-1051	0.00	Very wet	0.00
Southeast	0.44				
Southwest	0.98	Curvature			
West	0.71	Concave	1.09		
Northwest	1.42	Flat	0.85		
North	3.01	Convex	1.43		

Table 1. Computed frequency ratio for each factor.

The FR model indicated that landslide occurrences are most strongly associated with mid-elevation ranges: 210-410 meters (FR=1.95) and 410-610 meters (FR=3.16). This pattern is consistent with numerous studies showing that landslides tend to cluster at mid-elevations rather than at the highest or lowest parts of the landscape. Huang et al. (2022) found that nearly all landslides occurred between 500 and 1,500 meters elevation, with landslide frequency values greater than or close to one. Similarly, Gemitz et al. (2011) observed the highest landslide frequency between 200 and 900 meters, with a marked decline above 900 meters. This distribution is often linked to steep slopes, active erosion, and human activity at mid-elevations, while higher elevations tend to have more stable, rock-dominated slopes less prone to failure (Cellek, 2020).

The TWI results were somewhat unexpected, with the lowest TWI class (very dry) exhibiting the highest FR value of 2.09. This contradicts the common understanding that higher TWI values, indicative of wetter conditions, increase landslide susceptibility due to reduced soil shear strength from saturation (Parra et al., 2023). However, Bhadiyadra and Ong (2024) found that both excessively dry and wet conditions can compromise soil stability. In dry conditions, insufficient moisture reduces particle bonding and weakens the soil, increasing the chance of slope failure, while overly wet conditions weaken soil by reducing shear strength and eliminating soil suction. The results reveal how soil moisture strongly affects slope stability, stressing the importance of accounting for different moisture levels in landslide risk studies.

Aspect analysis revealed that slopes facing North, Northeast and South have FR values exceeding one (3.01, 1.97, and 1.42, respectively), indicating higher landslide susceptibility on these orientations. This likely reflects the combined effects of local rainfall patterns, slope steepness, and land use practices. Rodriguez-Caballero et al. (2021) similarly reported that most landslides occurred on steep north and northwest-facing slopes. Nevertheless, aspect's influence on landslide occurrence can vary regionally, shaped by local climatic and geological conditions.

### 3.2 Application of Logistic Regression

In logistic regression, the coefficients measure how each conditioning factor relates to landslide occurrence, which is the dependent variable (Chowdhury et al., 2024). A coefficient indicates the change in log-odds of a landslide for every one-unit rise in a given factor, assuming all other variables stay constant.

Curvature has a positive coefficient of 1.117 with an odds ratio of approximately 3.06, indicating that higher curvature values increase the likelihood of landslides. In contrast, TPI has a negative coefficient of -3.438 and an odds ratio of about 0.03, suggesting that higher TPI values are associated with a decreased landslide probability. TWI shows a small positive coefficient of 0.081 and an odds ratio near 1.08, implying a slight increase in landslide risk with increasing wetness index.

Causal Factor	Coefficient	Odds Ratio
Curvature	1.12	3.06
TPI	-3.44	0.03
TWI	0.08	1.08
Slope	9.57	14384.33
Elevation	1.15	3.15
Aspect	0.72	2.05
Soil Texture	4.70	110.48
Intercept	-2.33	0.097

Table 2. Regression coefficients for the seven causal factors.

The model is most influenced by slope steepness, showing a very high coefficient 9.574 and an odds ratio of approximately 14,384, underscoring its dominant effect on landslide susceptibility. This is consistent with established studies showing that steeper slopes experience greater gravitational stress, increasing failure probability (Tseng et al., 2017). Elevation and aspect have positive coefficients of 1.146 and 0.718, with odds ratios of about 3.15 and 2.05 respectively, indicating moderate influences on landslide occurrence. Soil texture also strongly affects landslide susceptibility, with a coefficient of 4.705 and an odds ratio of approximately 110.48, consistent with studies emphasizing the soil properties as key to slope stability (Sidle and Ochiai, 2006).

An intercept value of -2.33 gives the log-odds of landslide with all variables at zero or at their reference levels. This corresponds to a low baseline probability (odds ratio ~0.097), indicating that in the absence of conditioning factors, landslides are unlikely.

### 3.3 Landslide Susceptibility Map

A map is created by classifying LSI scores into classes. While common boundary rules guide reclassification, there is no consensus among researchers on a standard approach. As a result, class boundaries are often chosen by researcher's own expert judgement. (Gulbet and Getahun, 2024).

Using the manual classifier from Thanh et al. (2022), the LSM was grouped into low, moderate, high and very high

susceptibility. This is based on the rule that each higher category should account for roughly twice the number of landslide events as the one beneath it.

For the FR model, landslides are expected to distribute as 7.6% in low, 15.3% in moderate, 30.7% in high, and 46.4% in very high zones. On the other hand, the LR has an establish cut-off points at 7.69%, 23.07%, and 46.15%. These thresholds separate the four susceptibility classes for both methods, ensuring that the classification reflects the actual distribution of landslide events and provides a logical, data-driven basis for identifying areas at greatest risk.

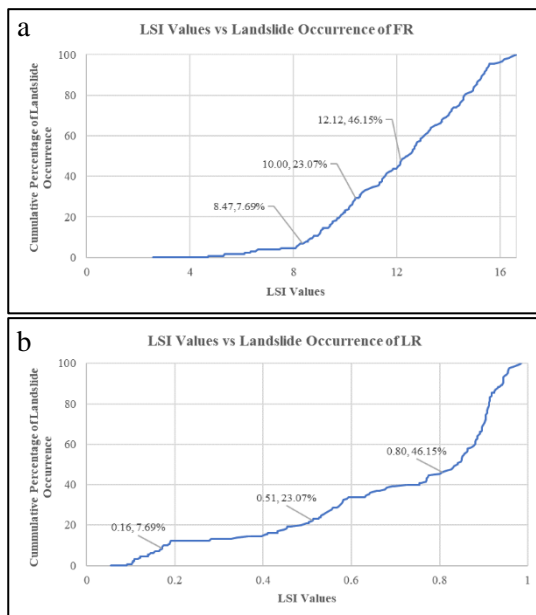


Figure 5. Relationship between landslide occurrence and LSI values derived from FR (a) and (b) LR.

Employing this categorization method, the thresholds for each susceptibility zone are shown in Table 3 (FR) and Table 4 (LR). Low susceptibility covers 69.20% of the area, indicating most places are unlikely to experience landslide. Moderate and high zones cover 10.73% and 10.66% of the area, respectively. Meanwhile, very high susceptibility comprises 9.41% of the area, highlighting specific regions that may require focused monitoring and mitigation efforts. Overall, more than 30% of the area falls in elevated-susceptibility zones, warranting targeted attention in future land-use planning and hazard reduction strategies.

Susceptibility	LSI Range	Area (ha)	Percent
Low	02.57 - 08.47	330,194.76	69.20
Moderate	08.47 - 10.00	51,207.66	10.73
High	10.00 - 12.12	50,861.64	10.66
Very high	12.12 - 16.61	44,897.36	9.41

Table 3. LSI ranges for susceptibility zones of Frequency Ratio (FR) and area distribution per susceptibility class.

Low susceptibility covers 54.74% of the area, indicating a generally low landslide chance across more than half of the landscape. 38.51% falls into the moderate category, suggesting a substantial portion of the region experiences a moderate level of landslide risk. In contrast, only 6.58% and 0.58% of the region covers the high and very high susceptibility categories respectively. These zones highlight smaller yet critical areas with

a significantly elevated potential for landslides, where monitoring and mitigation efforts should be concentrated.

Susceptibility	LSI Range	Area (ha)	Percent
Low	0.00-0.16	265,866.77	54.74
Moderate	0.16-0.51	187,026.68	38.51
High	0.51-0.80	29,968.26	06.58
Very high	0.80-1.00	2,814.04	00.58

Table 4. LSI ranges for susceptibility zones of Logistic Regression (LR) and area distribution per susceptibility class.

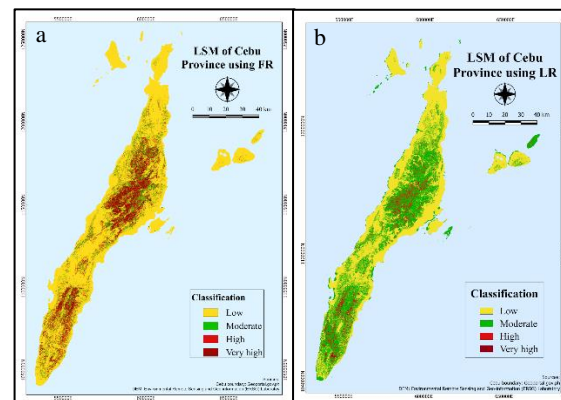


Figure 6. Landslide susceptibility maps (a) FR and (b) LR.

### 3.4 Model Validation

ROC curves compare the performance of FR and LR for both success and prediction rates. In both cases, the LR model demonstrates slightly superior performance, indicated by higher AUC values: 0.9120 versus 0.8850 for success rate, and 0.9434 versus 0.9249 for prediction rate. This shows that while both models exhibit good discriminatory power, the LR model has a modestly better ability to distinguish between classes and provide better predictions.

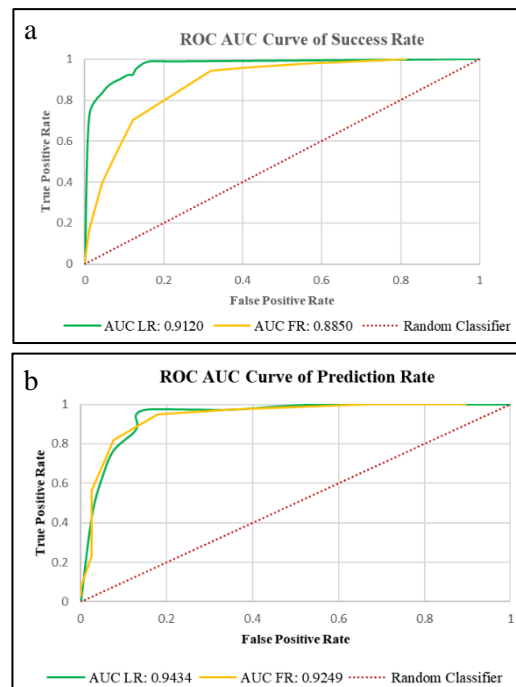


Figure 7. Success (a) and prediction (b) rate of FR and LR models.

Despite using the same set of conditioning factors in both models, the LR model in this study demonstrated marginally better discriminatory ability compared to the FR model. This difference likely stems from methodological distinctions: LR considers multivariate interactions among variables, whereas FR evaluates each factor independently.

This finding aligns with previous studies conducted in the Philippines. For example, Javier and Kumar (2019) reported a prediction rate of 89% using the FR for landslide susceptibility in Benguet Province. Similarly, Victor and Zarco (2018) found the LR model obtained an AUC of 0.908 in their study of Antipolo, Rizal. These results suggest that both methods perform well within the Philippine context; however, the LR model can capture complex interactions between conditioning variables, it may perform better in regions with diverse geological and climatic settings, such as the present study site.

From the recorded landslide data, most landslide events occurred in the central part of Cebu, particularly in the Municipality of Balamban and Cebu City. Landslides were also recorded in neighboring municipalities such as Asturias, Danao City, parts of Toledo City, Talisay City, and Minglanilla. Additionally, landslide events were reported in Aloguinsan. In the southern part of Cebu Province, Alegria recorded the greatest number of landslides, with occurrences also noted in Badian, Argao, Alcantara, Dalaguete, and Boljoon. These municipalities also fall under the high susceptibility class of MGB (MGB 7, n.d.).

### 3.5 Comparison of the produced LSM from MGB susceptibility map

A spatial comparison was performed between the LR-derived LSM and the MGB map. Table 6 shows the area distribution per susceptibility class of MGB landslide hazard map. The moderate class is largest at 40.21%, followed by high (34.86%), low (23.01%), and very high (1.92%). In contrast, the LR map classifies about half of the province falls under the low susceptibility class. This difference is illustrated in Figure 7, which highlights the agreement zones areas where both maps classify landslide risk similarly and the disagreement zones, where classifications differ. According to Table 7, 58.72% of the study area consists of agreement zones, while 41.27% consists of disagreement zones.

Susceptibility Zone	Area (ha)	Percent
Low	101,270.2	23.01
Moderate	176,942.4	40.21
High	153,391	34.86
Very high	8,438.74	01.92

Table 5. Spatial distribution of susceptibility zones from MGB.

An agreement map was generated to clearly identify areas where the two classifications match and mismatch. The comparison revealed notable differences: although both maps use four susceptibility zones, MGB covers a larger portion of the province to high and very high classes, while these classes appear more localized in the LR based map. These discrepancies may result from differences in input data, methodology, scale, and classification criteria. Additionally, a table summarizing the area of each susceptibility zone in the MGB map was compiled to quantitatively compare with the corresponding zones in the LR map. This combined approach enables both spatial and statistical evaluation of the similarities and differences between the two susceptibility assessments.

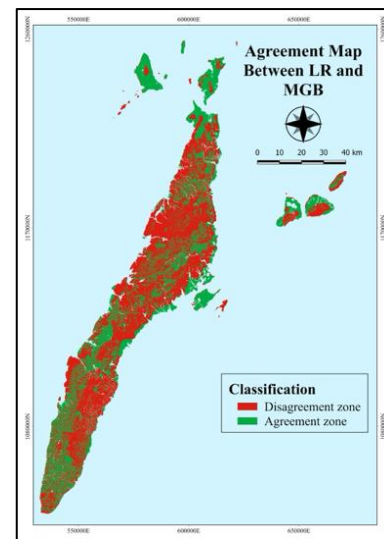


Figure 8. Agreement map between LR and MGB.

The primary reason for the observed differences between the landslide susceptibility maps lies in the distinct modelling approaches employed. While the map produced in this study uses LR model, the MGB map does not provide detailed information regarding the specific modelling technique used to generate their susceptibility classification. Additionally, variation in number and which factors are used strongly affect the final susceptibility results. This study incorporates only seven static factors, whereas the MGB map may include additional dynamic or environmental factors such as land use/land cover (LULC), rainfall intensity, proximity to rivers, and other relevant variables. Differences in input data quality, resolution, and the weighting or integration methods applied to these factors further contribute to variations in spatial patterns and susceptibility class extents. Together, these differences in modelling approach, factor selection, and data quality is a key factor influencing the differences observed between the two susceptibility maps.

Zone	Area (ha)
Agreement	257,142.11
Disagreement	180,716.35

Table 6. Spatial agreement between LR and MGB LSM.

### 4. Conclusion

The marginal improvement in LR performance highlights the value of incorporating multivariate relationships in landslide susceptibility mapping. This approach can enhance hazard assessment accuracy and support more effective risk management strategies. Future research could focus on integrating additional conditioning factors or exploring hybrid modeling techniques to further improve predictive performance.

The susceptibility maps from this study give a scientific basis for local government units and stakeholders to enhance plan for disasters, shape land use, and focus mitigation in Cebu Province. Future studies are encouraged to incorporate additional dynamic factors like rainfall and land-use change, and to explore advanced modelling techniques for even more robust hazard assessment.

### References

Arizapa, J.L., Combalicer, E.A., Tiburan, C.L. 2015. Landslide susceptibility mapping of Pagsanjan-Lumban Philippines

watershed using GIS and analytical hierarchy process. *Ecosystems & Development Journal*, 23–32.

Beroya-Eitner, M.A.A., Vicente, M.C.T.M., Dado, J.M.B., Dimain, M.R.S., Maquiling, J.T., Cruz, F.A.T. 2023. Climate Change as Modifier of Landslide Susceptibility: Case Study in Davao Oriental, Philippines. In: Alcántara-Ayala, I., et al. *Progress in Landslide Research and Technology*, Volume 2 Issue 2, 2023. *Progress in Landslide Research and Technology*. Springer, Cham. [https://doi.org/10.1007/978-3-031-44296-4\\_12](https://doi.org/10.1007/978-3-031-44296-4_12)

Bhadiyadra, K., Ong, D. E. L. 2024. Mechanics of Rainfall-Induced Landslides after a Prolonged Dry Period Based on Laboratory Tests and Numerical Models Incorporating Soil-Water Characteristic Curves. *Geosciences*, 14(7), 174. <https://doi.org/10.3390/geosciences14070174>

Blaga, L. 2012. Aspects regarding the significance of the curvature types and values in the studies of geomorphometry assisted by GIS. *Analele Universității Din Oradea, Seria Geografie*, 2, 327–337.

Bollettino, V., Alcayna, T., Enriquez, K., & Vinck, P. (2018) Perceptions of disaster resilience and preparedness in the Philippines. *Harvard Humanitarian Initiative, Harvard University*.

Cabelin, J., Jadina, B. 2019. Physical characteristics of soils in the landslide areas of Cadac-an Watershed in Leyte, Philippines. *Annals of Tropical Research/Annals of Tropical Research (Visayas State University-Online)*, 115–129. <https://doi.org/10.32945/atr4129.2019>

Çellek, S. 2020. Effect of the Slope Angle and Its Classification on Landslide. *Nat. Hazards Earth Syst. Sci. Discuss.* <https://doi.org/10.5194/nhess-2020-87>

Chang, L., Xing, G., Yin, H., Fan, L., Zhang, R., Zhao, N., Huang, F., Ma, J. 2023. Landslide susceptibility evaluation and interpretability analysis of typical loess areas based on deep learning. *Natural Hazards Research*, 3 (2), 155–169. <https://doi.org/10.1016/j.nhres.2023.02.005>

Chowdhury, S., Rahman, N., Sheikh, S., Sayeid, A., Mahmud, K.H., Hafsa, B. 2024. GIS-based landslide susceptibility mapping using logistic regression, random forest and decision and regression tree models in Chattogram District, Bangladesh. *Heliyon* 10 (2024) e23424. <https://doi.org/10.1016/j.heliyon.2023.e23424>

Das, G., Lepcha, K. 2019. Application of logistic regression (LR) and frequency ratio (FR) models for landslide susceptibility mapping in Relli Khola river basin of Darjeeling Himalaya, India. *SN Applied Sciences*, 1(11). <https://doi.org/10.1007/s42452-019-1499-8>

Fu, Y., Fan, Z., Li, X., Wang, P., Sun, X., Ren, Y., & Cao, W. (2025). The influence of Non-Landslide sample selection methods on landslide susceptibility prediction. *Land*, 14(4), 722. <https://doi.org/10.3390/land14040722>

Gemitzi, A., Falalakis, G., & Petalas, C. 2011. Evaluating landslide susceptibility using environmental factors, fuzzy membership functions and GIS. *Global NEST Journal*, 13(1), 28–40. <https://doi.org/10.30955/gnj.000734>

Gorokhovich, Y., & Vustianiuk, A. 2021. Implications of slope aspect for landslide risk assessment: A case study of Hurricane Maria in Puerto Rico in 2017. *Geomorphology*, 391, 107874. <https://doi.org/10.1016/j.geomorph.2021.107874>

Gulbet, E., Getahun, B. 2024. Landslide susceptibility mapping using frequency ratio and analytical hierarch process method in awabel woreda, ethiopia. *Quaternary Science Advances*, 100246. <https://doi.org/10.1016/j.qsa.2024.100246>

Huang, J., Zeng, X., Ding, L., Yin, Y., Li, Y. 2022. Landslide susceptibility evaluation using different slope units based on BP neural network. *Computational Intelligence and Neuroscience*, 2022, 1–15. <https://doi.org/10.1155/2022/9923775>

Javier, D.N., & Kumar, L. 2019. Frequency Ratio and Landslide Susceptibility Estimation in a Tropical Mountain Region. *International Archives of the Photogrammetry, Remote Sensing and Spatial Information Sciences*. <https://doi.org/10.5194/isprs-archives-xlii-3-w8-173-2019>

Jones, J.N., Bennett, G.L., Abancó, C., Matera, M.A.M., Tan, F.J. 2023. Multi-event assessment of typhoon-triggered landslide susceptibility in the Philippines. *Natural Hazards and Earth System Sciences*, 23(3), 1095–1115. <https://doi.org/10.5194/nhess-23-1095-2023>

Kinde, M., Getahun, E., Jothimani, M. 2024. Geotechnical and slope stability analysis in the landslide-prone area: A case study in Sawla – Laska road sector, Southern Ethiopia. *Scientific African*, 23, e02071. <https://doi.org/10.1016/j.sciaf.2024.e02071>

Liao, M., Wen, H., & Yang, L. 2022. Identifying the essential conditioning factors of landslide susceptibility models under different grid resolutions using hybrid machine learning: A case of Wushan and Wuxi counties, China. *CATENA*, 217, 106428. <https://doi.org/10.1016/j.catena.2022.106428>

Mines and Geosciences Bureau-7. 2019. Cebu Province Mineral Profile. Retrieved April 26, 2025, from <https://r7.mgb.gov.ph/wp-content/uploads/2020/06/Cebu-Regional-Profile-2019.pdf>

Meles, M. B., Younger, S. E., Jackson, C. R., Du, E., & Drover, D. 2019. Wetness index based on landscape position and topography (WILT): Modifying TWI to reflect landscape position. *Journal of Environmental Management*, 255, 109863. <https://doi.org/10.1016/j.jenvman.2019.109863>

Rodriguez-Caballero, E., Rodriguez-Lozano, B., Segura-Tejada, R., Blanco-Sacristán, J., & Cantón, Y. 2021. Landslides on dry badlands: UAV images to identify the drivers controlling their unexpected occurrence on vegetated hillslopes. *Journal of Arid Environments*, 187, 104434. <https://doi.org/10.1016/j.jaridenv.2020.104434>

Sidle, R. C., Ochiai, H. 2006. Landslides: processes, prediction, and land use. In Water resources monograph. <https://doi.org/10.1029/wm018>

Silalahi, F. E. S., Pamela, N., Arifianti, Y., Hidayat, F. 2019. Landslide susceptibility assessment using frequency ratio model in Bogor, West Java, Indonesia. *Geoscience Letters*, 6(1). <https://doi.org/10.1186/s40562-019-0140-4>

Shabbir, W., Omer, T., Pilz, J. 2022. The impact of environmental change on landslides, fatal landslides, and their

triggers in Pakistan (2003–2019). *Environmental Science and Pollution Research International*, 30(12), 33819–33832. <https://doi.org/10.1007/s11356-022-24291-z>

Sharma, A., Sandhu, H. a. S. 2024. Investigating the dynamic nature of landslide susceptibility in the Indian Himalayan region. *Environmental Monitoring and Assessment*, 196(3). <https://doi.org/10.1007/s10661-024-12440-5>

Sheng, M., Zhou, J., Chen, X., Teng, Y., Hong, A., Liu, G. 2022. Landslide susceptibility prediction based on frequency ratio method and C5.0 Decision Tree model. *Frontiers in Earth Science*, 10. <https://doi.org/10.3389/feart.2022.918386>

Shano, L., Raghuvanshi, T. K., Meten, M. 2020. Landslide susceptibility evaluation and hazard zonation techniques – a review. *Geoenvironmental Disasters*, 7(1). <https://doi.org/10.1186/s40677-020-00152-0>

Sonker, I., Tripathi, J. N., Singh, A. K. 2021. Landslide susceptibility zonation using geospatial technique and analytical hierarchy process in Sikkim Himalaya. *Quaternary Science Advances*, 4, 100039. <https://doi.org/10.1016/j.qsa.2021.100039>

Sun, X., Chen, J., Bao, Y., Han, X., Zhan, J., Peng, W. 2018. Landslide Susceptibility Mapping Using Logistic Regression Analysis along the Jinsha River and Its Tributaries Close to Derong and Deqin County, Southwestern China. *ISPRS Int. J. Geo-Inf.* 2018, 7, 438; doi:10.3390/ijgi7110438

Thanh, L. N., Fang, Y., Chou, T., Hoang, T., Nguyen, Q. D., Lee, C., Wang, C., Yin, H., Lin, Y. 2022. Using Landslide Statistical Index Technique for landslide susceptibility mapping: Case study: Ban Khoang Commune, Lao Cai Province, Vietnam. *Water*, 14(18), 2814. <https://doi.org/10.3390/w14182814>

Temme, A. J. 2021. Relations between soil development and landslides. *Geophysical Monograph*, 177–185. <https://doi.org/10.1002/9781119563952.ch9>

Tseng, CH., Chan, YC., Jeng, CJ. 2017. Slip monitoring of a dip-slope and runout simulation by the discrete element method: a case study at the Huafan University campus in northern Taiwan. *Nat Hazards* 89, 1205–1225. <https://doi.org/10.1007/s11069-017-3016-y>

Umbara, R.P. 2024. Utilization of Frequency Ratio and Logistic Regression Model for Landslide Susceptibility Mapping in Bogor Area. *Int. J. Adv. Sci. Eng. Inf. Technol.*, vol. 14, no. 2, pp. 528–539

Vasudevan, N., Ramanathan, K. 2016. Geological factors contributing to landslides: case studies of a few landslides in different regions of India. *IOP Conference Series Earth and Environmental Science*, 30, 012011. <https://doi.org/10.1088/1755-1315/30/1/012011>

Victor, J.A., & Zarco, M.A., 2018. Multivariate Logistic Regression Approach for Landslide Susceptibility Assessment of Antipolo, Rizal. *Philippine Engineering Journal*, [S.I.], v. 39, n. 2, dec. 2018. ISSN 2718-9287.

Weiss, A. 2001. Topographic Position and Landforms Analysis. Poster Presentation, ESRI User Conference, San Diego, 9-13 July 2001.

Wubalem, A. 2021. Landslide susceptibility mapping using statistical methods in Uatzau catchment area, northwestern Ethiopia. *Geoenvironmental Disasters* 8, 1. <https://doi.org/10.1186/s40677-020-00170-y>

Yao, Y., Fan, J., & Li, J. 2025. A review of advanced soil moisture monitoring techniques for slope stability assessment. *Water*, 17(3), 390. <https://doi.org/10.3390/w17030390>